



Published in final edited form as:

Otolaryngol Head Neck Surg. 2014 March ; 150(3): 441–447. doi:10.1177/0194599813516420.

The Periductal Channels of the Endolymphatic Duct, Hydrodynamic Implications

Fred H. Linthicum Jr, MD¹, Joni Doherty, MD, PhD¹, Paul Webster, PhD¹, and Andres Makarem, MD¹

¹House Research Institute, Los Angeles, California, USA

Abstract

Objective—To describe the anatomy of a small network of channels surrounding the human endolymphatic duct.

Study Design—Archival temporal bone sections and a surgical specimen were studied using a variety of techniques.

Setting—Temporal bone laboratory of the House Research Institute.

Subjects and Methods—Archival temporal bone sections were examined by light microscopy, 3D reconstruction, and immunohistochemical labeling. A surgical specimen was examined using electron microscopy. Sections from temporal bones with blocked endolymphatic ducts or amputated sacs were examined for the manifestations of endolymphatic hydrops.

Results—Peri-endolymphatic duct channels were found to extend from the proximal cisternal part of the endolymphatic sac to the supporting tissue of the saccule and utricle. Tissue in the channels, as seen by conventional and electron microscopy, is continuous with and identical with the tissue surrounding the endolymphatic duct. Tissue in the channels labels with the S100 antibody similar to the spiral ligament and supporting tissue of the vestibular end organs and suggests a neural crest origin, as did the presence of melanocytes. Obstruction of the endolymphatic duct resulted in endolymphatic hydrops whereas amputation of the sac did not.

Conclusion—Endolymph is probably absorbed in the endolymphatic duct. The peri-endolymphatic duct channels that extend from the proximal sac to the supporting tissue of the saccule label with the S100 antibody and contain melanocytes suggest a neural crest origin and involvement in fluid and potassium hydrodynamics similar to those described for the similarly staining spiral ligament of the cochlea.

Corresponding Author: Fred H. Linthicum Jr., MD, House Research Institute, 2122 West Third Street, Los Angeles CA, 90057, USA. flinthicum@mednet.ucla.edu.

This article was presented at the 2013 AAO-HNSF Annual Meeting & OTO EXPO; September 29–October 3, 2013; Vancouver, British Columbia, Canada.

Author Contributions

Fred H. Linthicum, Jr., conceived project, wrote original draft; Joni Doherty, immunohistochemistry labeling supervision, editorial revision; Paul Webster, endolymphatic duct dissection, thick section identification, and thin section electron microscopic analysis; Andres Makarem, analysis of 3D anatomy using sequential histologic sections and Amira 3D reconstruction software.

Disclosures

Competing interests: None.

Sponsorships: None.

Keywords

endolymphatic duct; channels

Introduction

Surrounding the human endolymphatic duct is a group of small channels that originate in the proximal cisternal area of the endolymphatic sac and terminate in the supporting tissue of the sacculle^{1,2} (Figures 1 and 2). A few of the channels contain small thin walled vessels that could be capillaries or lymphatics. These channels have received little attention in the literature, perhaps because they are not so prominent in the animals normally used for investigational purposes. The channel configuration and morphology suggest that they may be involved in fluid and electrolyte movement. In this study, we used light and electron microscopy, immunohistochemistry, and 3D reconstructions to clarify the morphology and functional histology of the periolymphatic duct channels.

Methods

Three groups of bones and 1 surgical specimen were used in this study: 12 bones for evidence of obstructed endolymphatic ducts, 7 for 3D reconstruction, and 5 for immunohistochemistry. The temporal bones used in this project were from patients of the House Clinic who had made pledges to the House Research Institute. They were removed intracranially and fixed in 10% buffered formalin for 1 month and then decalcified in ethylenediaminetetracetic acid (EDTA) for several months until shown by x-ray to be free of calcium. The specimens were then dehydrated in graded alcohols (80%, 95%, 100%) before being placed into increasing concentrations of celloidin (2%, 4%, 6%, and 12%). The celloidin blocks were cleared with cedar wood oil and then cut into 20 micron sections that were placed onto numbered tissue squares. Every tenth section was stained with hematoxylin and eosin (H&E) and mounted on 1 inch 3 3 inch glass slides. The remaining sections are stored on the numbered tissues in 80% ethanol and used as necessary for special evaluations such as 3D reconstructions or immunohistochemistry. The clinical and histopathological findings of each case were entered into a database that allows for the retrieval of combinations of specific clinical or histopathological data. For 3D reconstruction, every section containing the endolymphatic duct was stained and mounted onto glass slides. The process, previously described,^{3,4} uses Amira 4.1 (Mercury Computer Systems/TGS, San Diego, California) software that enables a 3D reconstruction of digital images using successive sections. A search of the database revealed 8 bones that had obstructed endolymphatic ducts and 4 with amputated endolymphatic sacs (Table 1). 3D Reconstructions were made of 7 cases, 2 on vertically cut bones. Structures of interest for immunohistochemical labeling were identified, in 5 cases, on the mounted H&E sections, and the stored sections were identified by the numbered tissues upon which they were stored. The retrieved sections were mounted on gelatin subbed glass slides, and celloidin removal was performed as described by O'Malley et al⁵ using freshly prepared sodium methoxide (50 mg NaOH pellets dissolved into 50 ml methanol and then mixed 1:2 with methanol). Sections were blocked with goat serum for 1 hour at room temperature and then

incubated with the following primary antibodies overnight at 4°C: anti-Prox1 (Temecula, California), podoplanin (Acris antibodies, San Diego, California), CD34 (BD Pharmingen, San Jose, California), CD105 (BD Pharmingen), neuropilin1 (angiogenesis promoter via VEGF), VEGFR3 (Abcam, Cambridge, Massachusetts). Breast cancer tissue samples were processed in parallel (as positive control for both blood and lymphatic vessel endothelial cells), and for both breast cancer tissue and temporal bone sections, negative controls were included by omitting the primary antibody. For electron microscopy, the bone containing the endolymphatic duct was excised from a patient during the translabyrinthine approach to a vestibular nerve schwannoma (St Vincent Medical Center IRB #06-030) (reviewed October 3, 2012).⁶ The specimen was immersed in glutaraldehyde and subsequently decalcified and prepared for electron microscopic evaluation. Images were made of the fibrocytes of the peri endolymphatic tissue and the channels for comparison of the fibrocyte morphology with a Tecnai-G220 electron microscope. Measurements of the endolymphatic duct length was made in 9 cases of Meniere's disease and 9 controls (Table 2).

Results

The 8 bones that were identified in the database had blocked endolymphatic ducts due to a variety of causes including an osteoma, syphilitic micro-gummata, scarlet fever, other nonspecific inflammations, or surgical interventions; all 8 had microscopic evidence of endolymphatic hydrops in the cochlea and saccule (Figures 3 and 4) (Table 1). Four bones in which the duct was left intact but had the endolymphatic sac amputated as a result of disease or surgery had no evidence of hydrops. Three-dimensional reconstruction of the periductile channels demonstrated that they surrounded the vestibular aqueduct from the proximal cisternal segment of the endolymphatic sac and became confluent with channels passing in the wall of the vestibule to the supporting tissue of the saccule and utricle (Figures 2 and 5). The channels occasionally penetrated the wall of the aqueduct to contact the tissue surrounding the endolymphatic duct (Figure 2). In a case of temporal bone fracture wherein the fracture extended to but not through the duct, there was a loss of channels on the side interrupted by the fracture and an increase in their number on the fracture-free side (Figure 4). The tissue within the channels was shown to have the same morphology, using light and electron microscopy and immunohistochemistry, as the tissue surrounding the endolymphatic duct within the aqueduct. In Figure 2 they are shown as different colors to make them distinguishable from the duct and to avoid confusion. Immunohistochemical labeling with S100 antibody and fast red chromogen of the periductal tissue and the channels manifest the same reaction as the cochlear spiral ligament (Figure 6). Fast red was used as the chromogen because the melanocytes found in the periductal tissue appear the same as cells labeled with the commonly used DAB chromogen. A few of the channels contained thin walled vessels that labeled with podoplanin, a marker for lymphatics, and fast red chromogen. Each of the few channels in the guinea pig contained a vessel and the surrounding tissue labeled with S100 as they did in the human (Figure 7). Electron microscopic examination of the specimen removed during surgery demonstrated that the fibrocytes in the periductal channels had the same morphology as those in the periductal tissue within the vestibular aqueduct (Figure 8). No statistical difference in the length of the

endolymphatic duct was found between cases of Meniere's disease and a similar number of controls (Table 2).

Discussion

The movement of endolymph from the cochlea into the endolymphatic duct and sac was first demonstrated by Guild⁷ using potassium ferrocyanide and iron-ammonium citrate injected into the cochlear duct and then microscopically observing the presence of precipitated ferrocyanide (Prussian Blue) in the sub-epithelium of endolymphatic sac of Rask-Andersen et al⁸ and demonstrate that the endolymph is absorbed in the endolymphatic duct rather than by the endolymphatic sac. It has also been proposed that potassium is absorbed by the duct by Miyamoto and Morgenstern.⁹ This hypothesis was supported by Silverstein¹⁰ who found a significant decrease in potassium concentration in the saccular endolymph compared to that in the cochlear duct. Since Hallpike and Cairns¹¹ and Yamanaka¹² first associated microscopic evidence of endolymphatic hydrops with the symptoms of Meniere's syndrome, many investigators have accepted the relationship as factual. Whether the hydrops seen in temporal bones from individuals with Meniere's disease is due to overproduction or malabsorption of endolymph has not been established. It would appear that the altered hydrodynamics that occurs in Meniere's syndrome are not related to the duct and channels, as we were unable to find any difference in the length or morphology between ducts from Meniere's disease and controls. Results of immunostaining with S-100 suggest a neural crest origin of the cells in the periductal channels, as well as the tissue surrounding the endolymphatic duct and sac similar to the cochlear spiral ligament (Figure 6). This is validated by the presence of melanocytes in the periductile tissue and some of the channels.^{13,14} The cells of the cochlear spiral ligament have been implicated in the recirculation of potassium necessary for normal hair cell function.¹⁵ The similarity of the cells in the periductal channels suggests they may also be involved in ion and possibly fluid transport. As described in the introduction, analysis of 12 temporal bones indicate that the endolymph is absorbed from the duct, as suggested by Friberg et al,¹⁶ and the configuration of the periductal channels suggests that they may be involved in ion and fluid movement. The periductile channels are apparently a dynamic system responsible to physiologic demands as exemplified by their disappearance in nonfunctioning ducts and their ability to compensate for an anatomical alteration (Figure 5). The determination that the periductal channels are contiguous with similar channels in the posterior wall of the vestibule that in turn are connected to the supporting tissue of the saccule (Figures 5 and 6) suggests that they may serve as a fluid or ion transporter system. Also the labeling by the S100 antibody, similar to the cochlear spiral ligament that has been implicated in ion transfer,¹³ is more evidence that the channels may play a part in endolymphatic hydrodynamics. Although the configuration and histology of the periductile channels suggest a role in fluid and electrolyte transport, their possible role in abnormal physiology of endolymphatic hydrodynamics is yet to be defined.

Acknowledgments

The authors wish to thank Jose Fayad, MD, and Celine Richard MD, PhD, for their assistance and guidance.

Funding source:

NIDCD/NIH (NIDCD U24 DC 011962-03), funding only.

References

1. Ng M, Linthicum FH Jr. Periductal vessels of the endolymphatic duct. *Acta Otolaryngol (Stockh)*. 1992; 112:649–657. [PubMed: 1442011]
2. Anna-Karin H, Hultgård-Ekwall AK, Couloigner V, Rubin K, Rask-Andersen H. Network organization of interstitial connective tissue cells in the human endolymphatic duct. *J Histochem Cytochem*. 2003; 51:1491–1500. [PubMed: 14566021]
3. Somdas MA, Li PM, Whiten DM, Eddington DK, Nadol JB Jr. Quantitative evaluation of new bone and fibrous tissue in the cochlea following cochlear implantation in the human. *Audiol Neurootol*. 2007; 12:277–284. [PubMed: 17536196]
4. Fayad JN, Makarem AO, Linthicum FH Jr. Histopathologic assessment of fibrosis and new bone formation in implanted human temporal bones using 3D reconstruction. *Otolaryngol Head Neck Surg*. 2009; 141:247–252. [PubMed: 19643260]
5. O'Malley JT, Burges BJ, Jones DD, Adams JC, Merchant SN. Techniques of celloidin removal from temporal bone sections. *Ann Otol Rhinol Laryngol*. 2009; 118:435–441. [PubMed: 19663375]
6. Danckwardt-Lillieström N, Rask-Andersen H, Linthicum FH, House WF. A technique to obtain and process surgical specimens of the human vestibular aqueduct for histopathological studies of the endolymphatic duct and sac. *ORL J Otorhinolaryngol Relat Spec*. 1992; 54:215–219. [PubMed: 1484705]
7. Guild SR. The circulation of the Endolymph. *Am J Anat*. 1927; 33:57–81.
8. Rask-Andersen H, Bredberg G, Lyttkens L, Löf G. The function of the endolymphatic duct—an experimental study using ionic lanthanum as a tracer: a preliminary report. *Ann N Y Acad Sci*. 1981; 374:11–19. [PubMed: 6951432]
9. Miyamoto H, Morganstern C. Potassium level in endolymphatic sac in guinea pigs in vivo. *Arch Otorhinolaryngol*. 1979; 222:77–78. [PubMed: 426726]
10. Silverstein H. Biochemical studies of the inner ear fluids in the cat. Preliminary report. *Ann Otol Rhinol Laryngol*. 1966; 75:48–63. [PubMed: 5929516]
11. Hallpike CS, Cairns H. Observations on the pathology of Meniere's syndrome: (Section of Otology). *Proc R Soc Med*. 1938; 31:1317–1336. [PubMed: 19991672]
12. Yamanaka K. Über die pathologische Veränderung bei einem Menierre Kranken. *J Otorhinolaryngol Soc Jpn*. 1938; 44:2310–2312.
13. Sommer L. Generation of melanocytes from neural crest cells. *Pigment Cell Melanoma Res*. 2011; 24:411–421. [PubMed: 21310010]
14. Gussen R. Melanocyte system of the endolymphatic duct and sac. *Ann Otol Rhinol Laryngol*. 1978; 87(2 Pt 1):175–179. [PubMed: 646284]
15. Spicer SS, Schulte BA. Differentiation of inner ear fibrocytes according to their ion transport related activity. *Hear Res*. 1991; 56:53–64. [PubMed: 1663106]
16. Friberg U, Rask-Andersen H, Bagger-Sjöbäck D. Human endolymphatic duct. An ultrastructural study. *Arch Otolaryngol*. 1984; 110:421–428. [PubMed: 6732582]

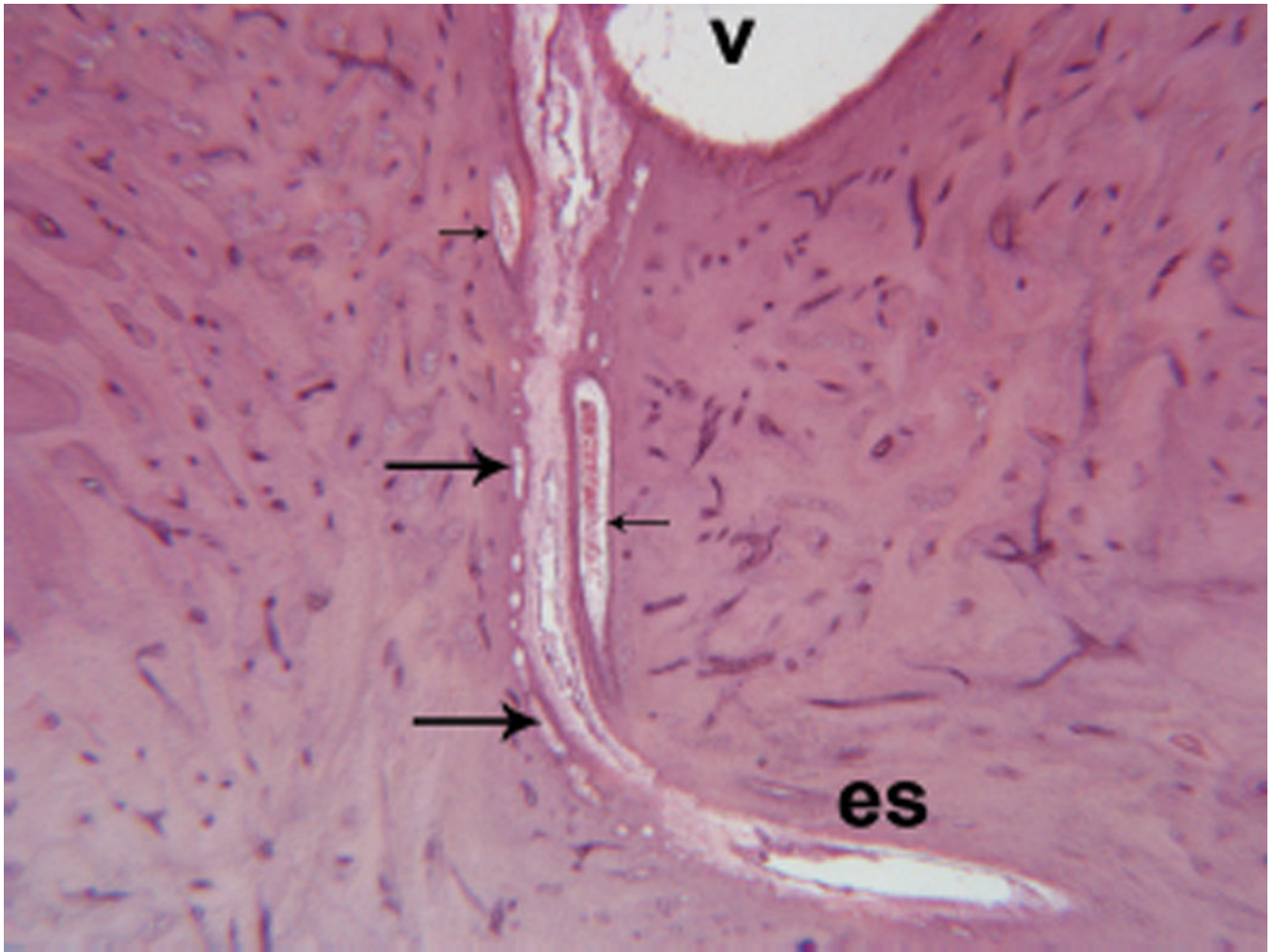


Figure 1. Endolymphatic duct surrounded by periductile channels (large arrows) extending from the vestibule (v) to the endolymphatic sac (es). Vein of the vestibular aqueduct (small arrows). (Hematoxylin and eosin [H&E] \times 20.)

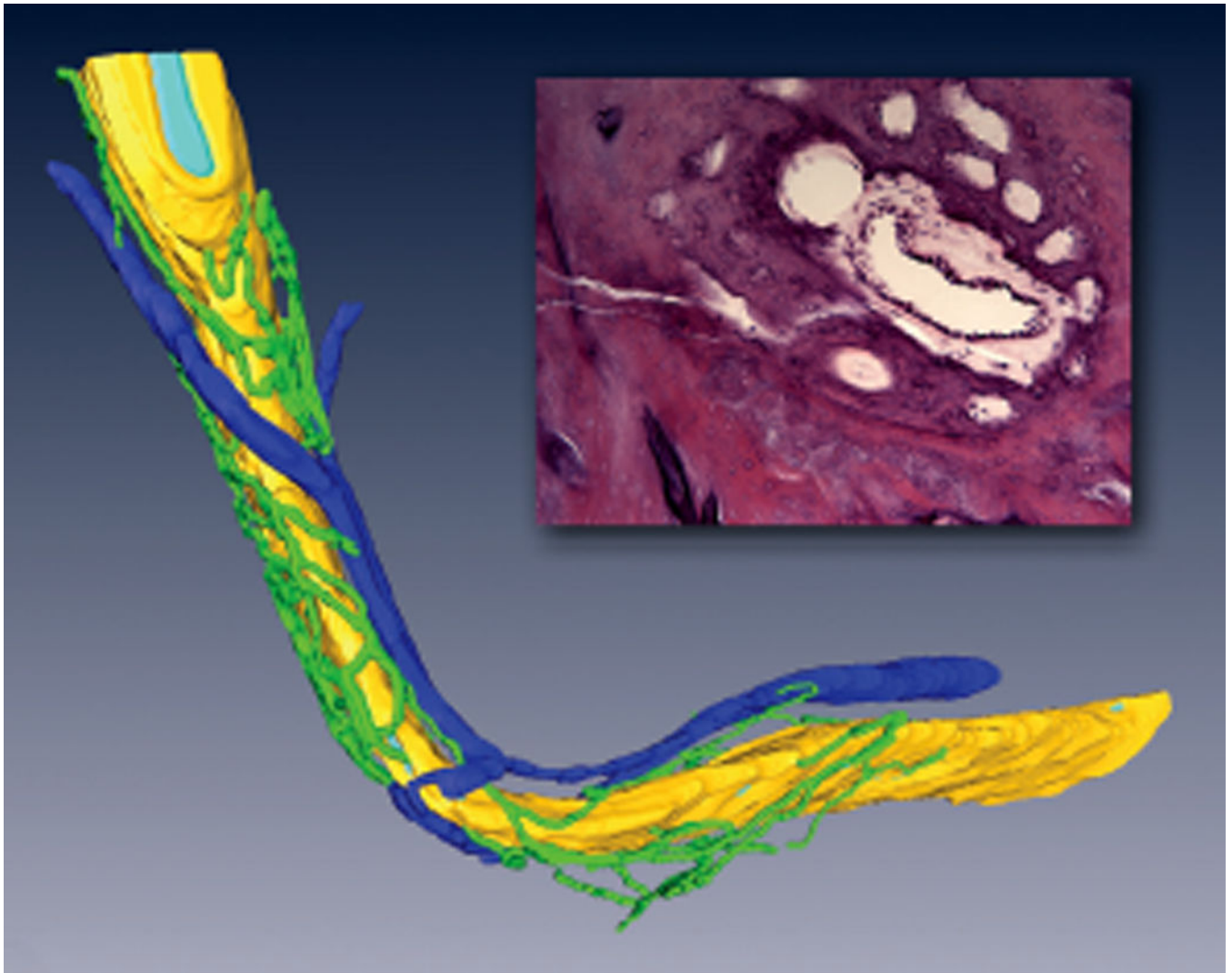


Figure 2. Three-dimensional reconstruction of periductile channels (green) surrounding the vestibular aqueduct (yellow) containing the endolymphatic duct (light blue) and a cross-section of the duct and surrounding periductile channels. Dark blue, periaqueductal vein.

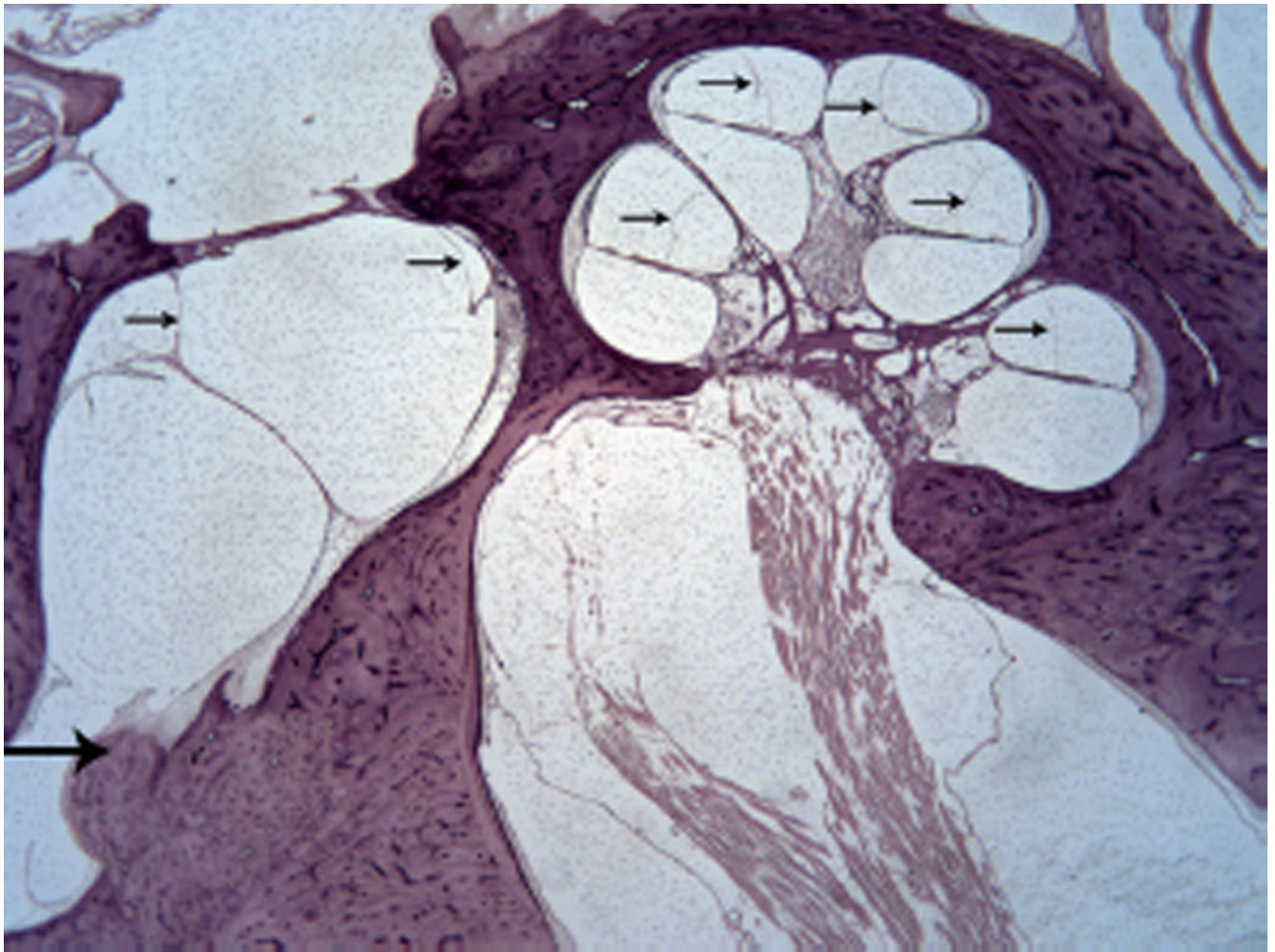


Figure 3. Endolymphatic duct obstructed by an osteoma (large arrow). Hydrops of the cochlear duct and saccule (small arrows). (Hematoxylin and eosin [H&E] $\times 10$.)

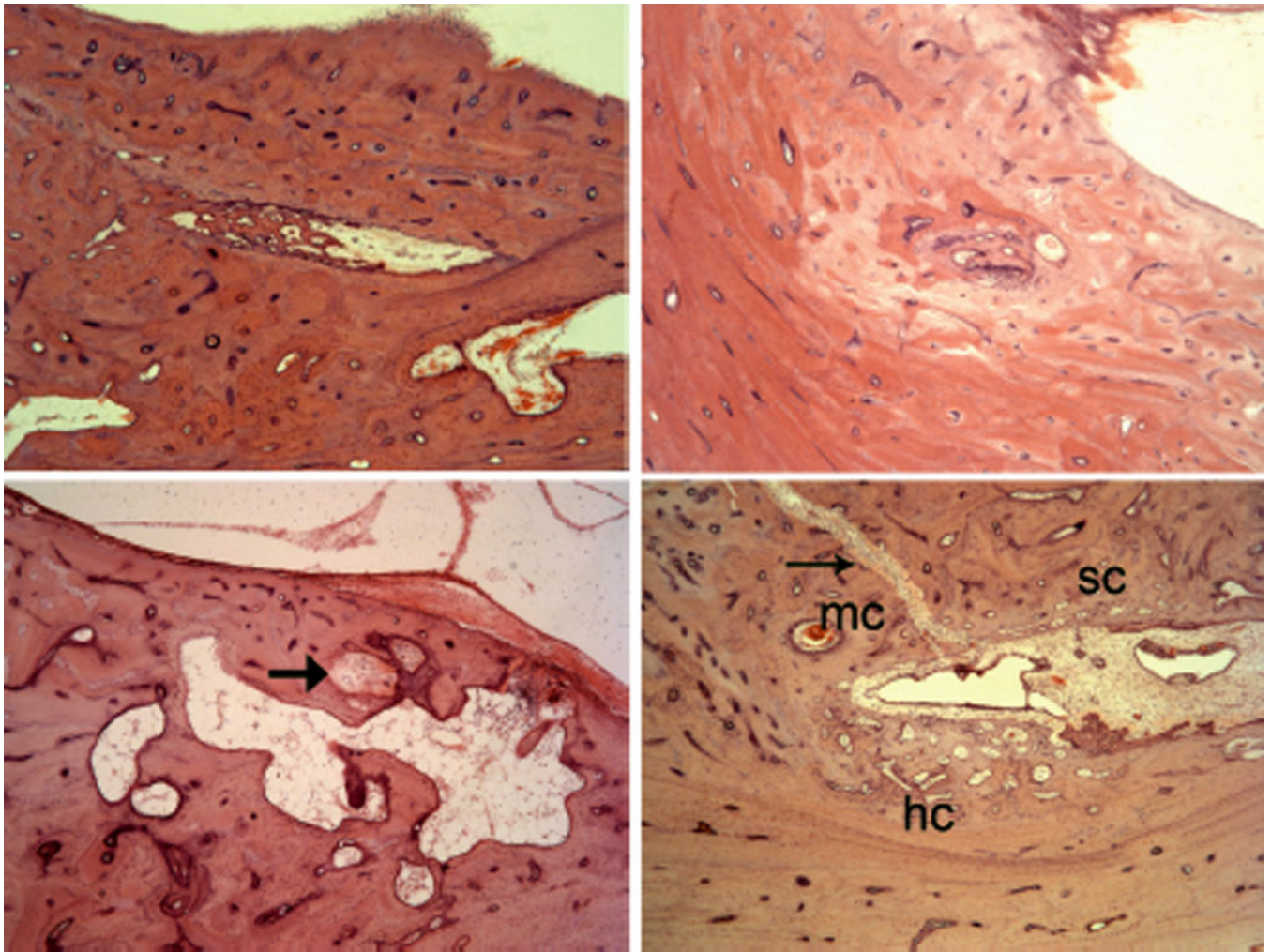


Figure 4. Obstructed endolymphatic ducts due to (upper left) scarlet fever, (upper right) nonspecific inflammation, (lower right) syphilitic microgumma. Lower right: Healed fracture (arrow) from vestibule to, but not through the duct. See text for details. (Hematoxylin and eosin [H&E] $\times 100$.)

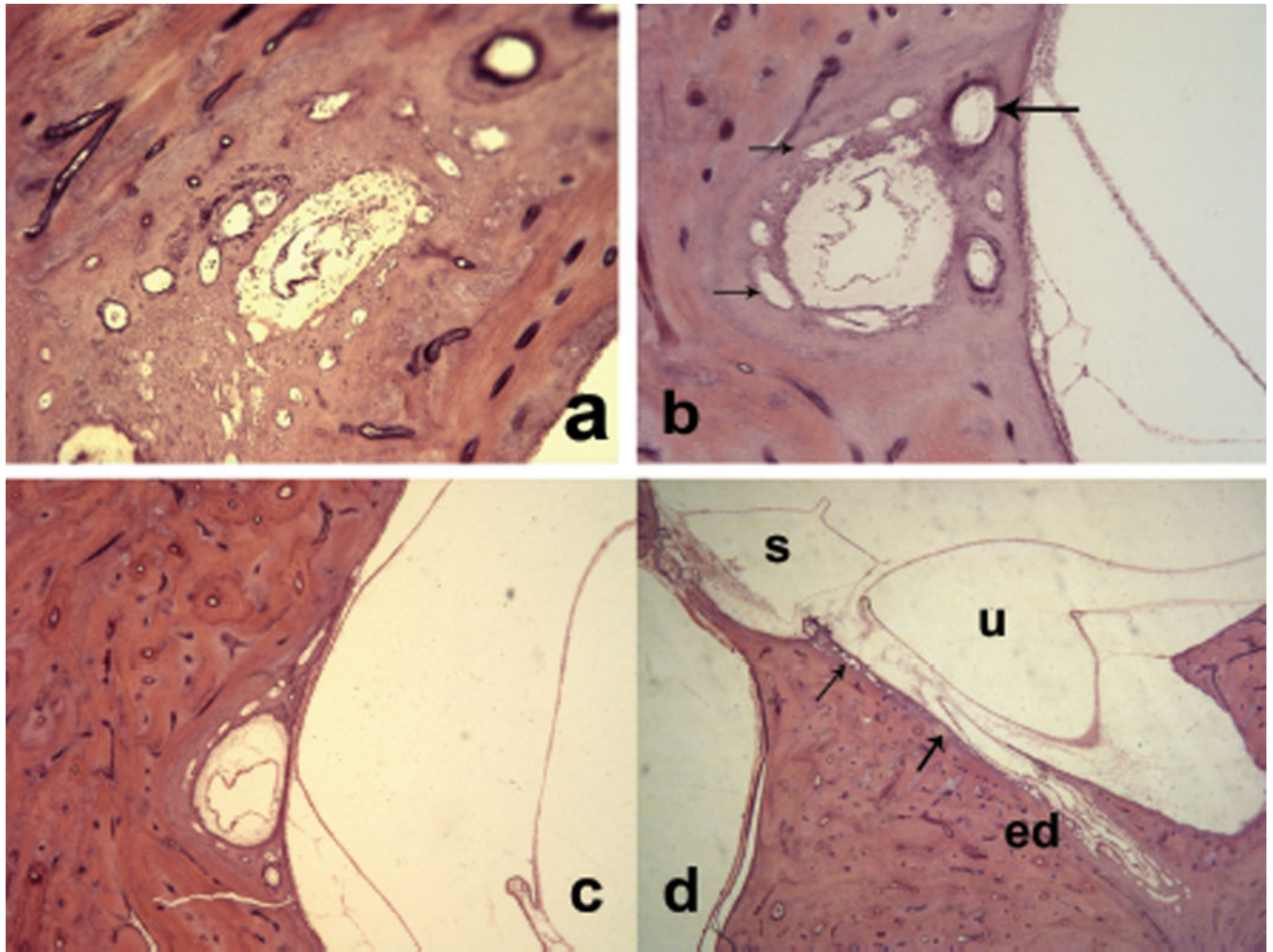


Figure 5. Sections through the endolymphatic duct, surrounded by periductile channels (small arrows) from (a) the distal portion to (d) the supporting tissue of the saccule. Large arrow indicates vein of the vestibular aqueduct.

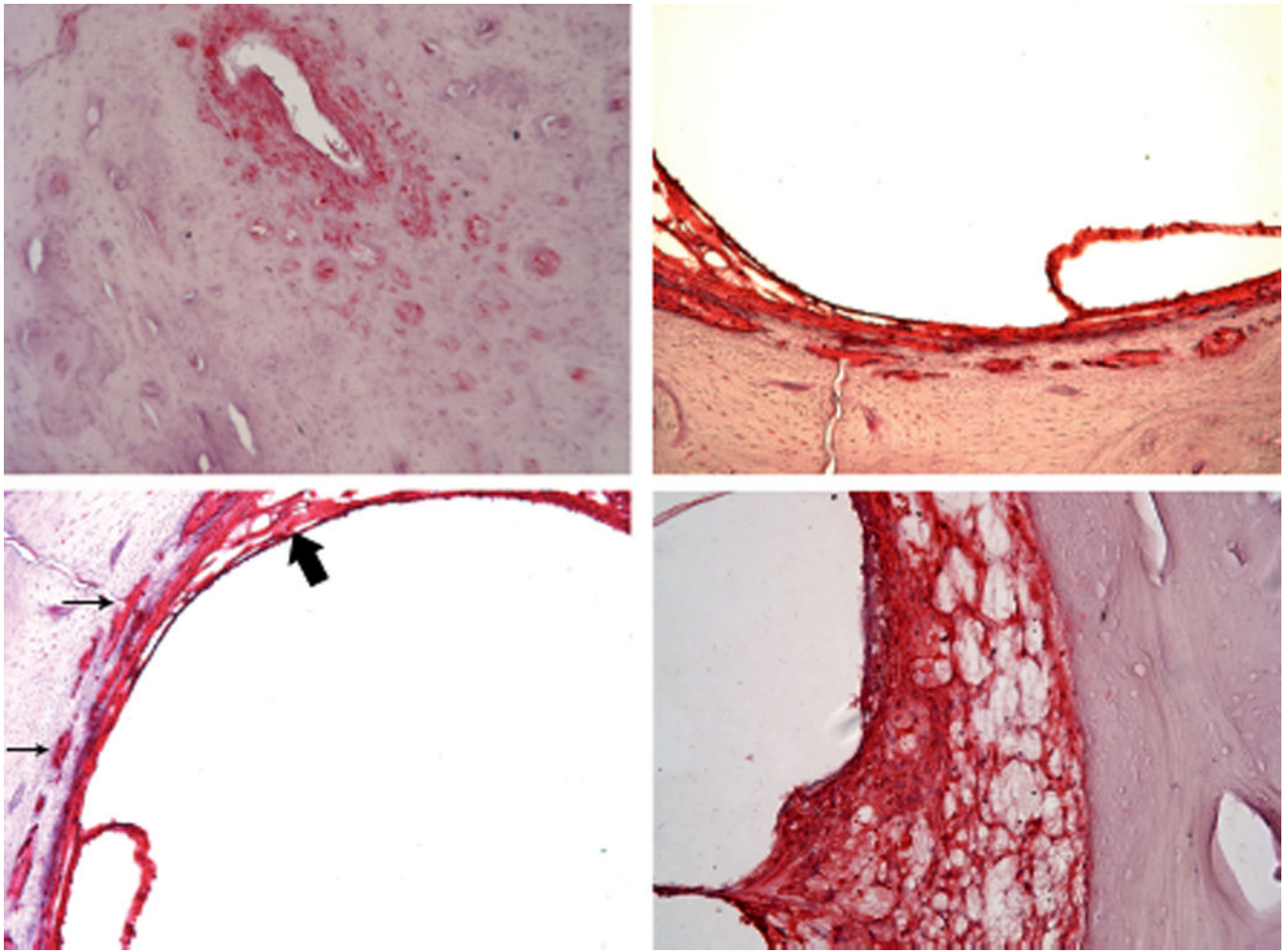


Figure 6. S100 antibody in periductile tissue and channels at (upper left) midpoint of duct, (upper right) wall of vestibule. Channels (small arrows) entering into (lower left) saccular supporting tissue (large arrows) and spiral ligament.

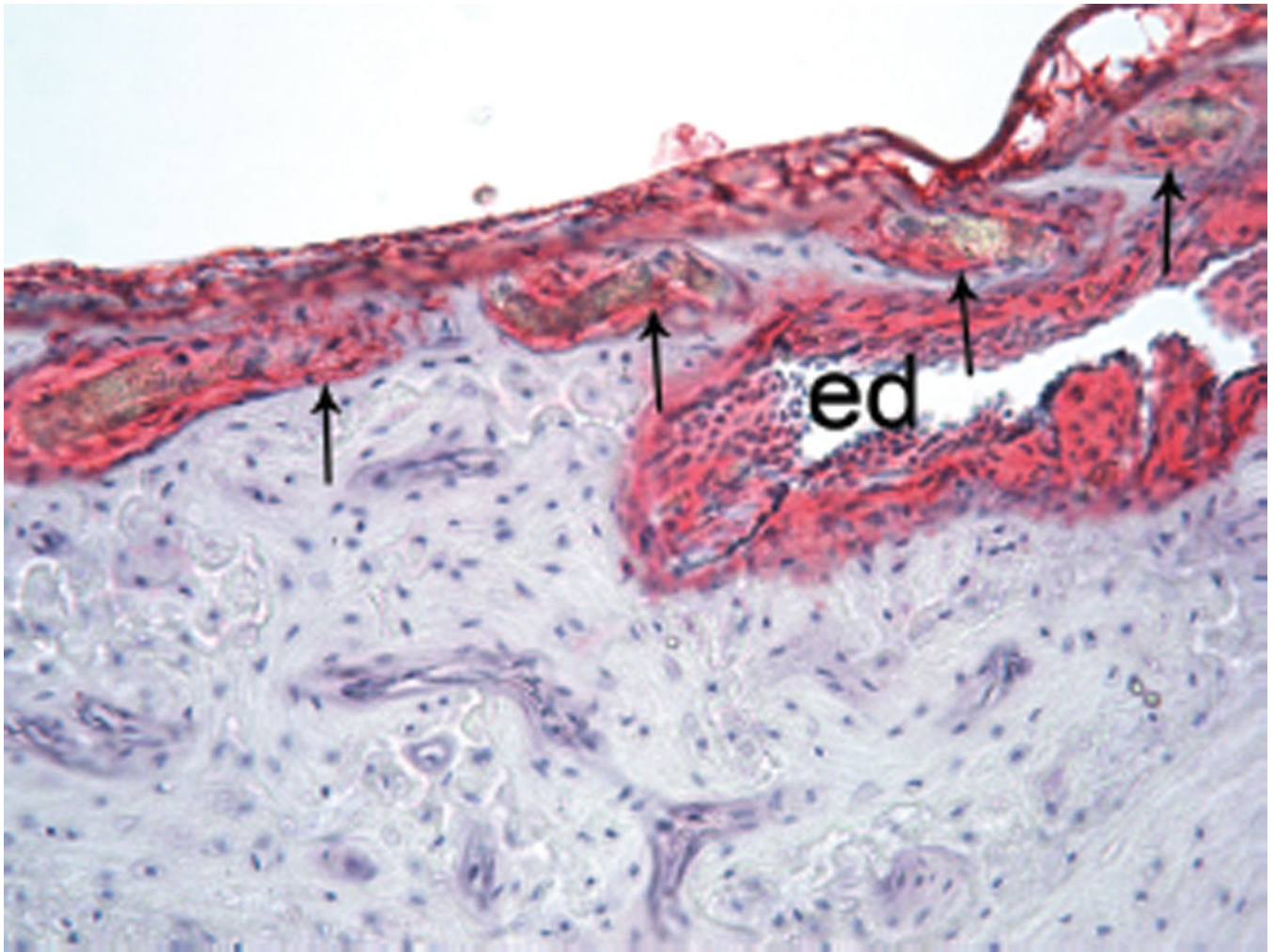


Figure 7. S100 labeling of endolymphatic duct (ed) and periductile channels (arrows) at junction of duct with the vestibule in a guinea pig. Some channels are around the duct and others are in the wall of the vestibule. ($\times 200$.)

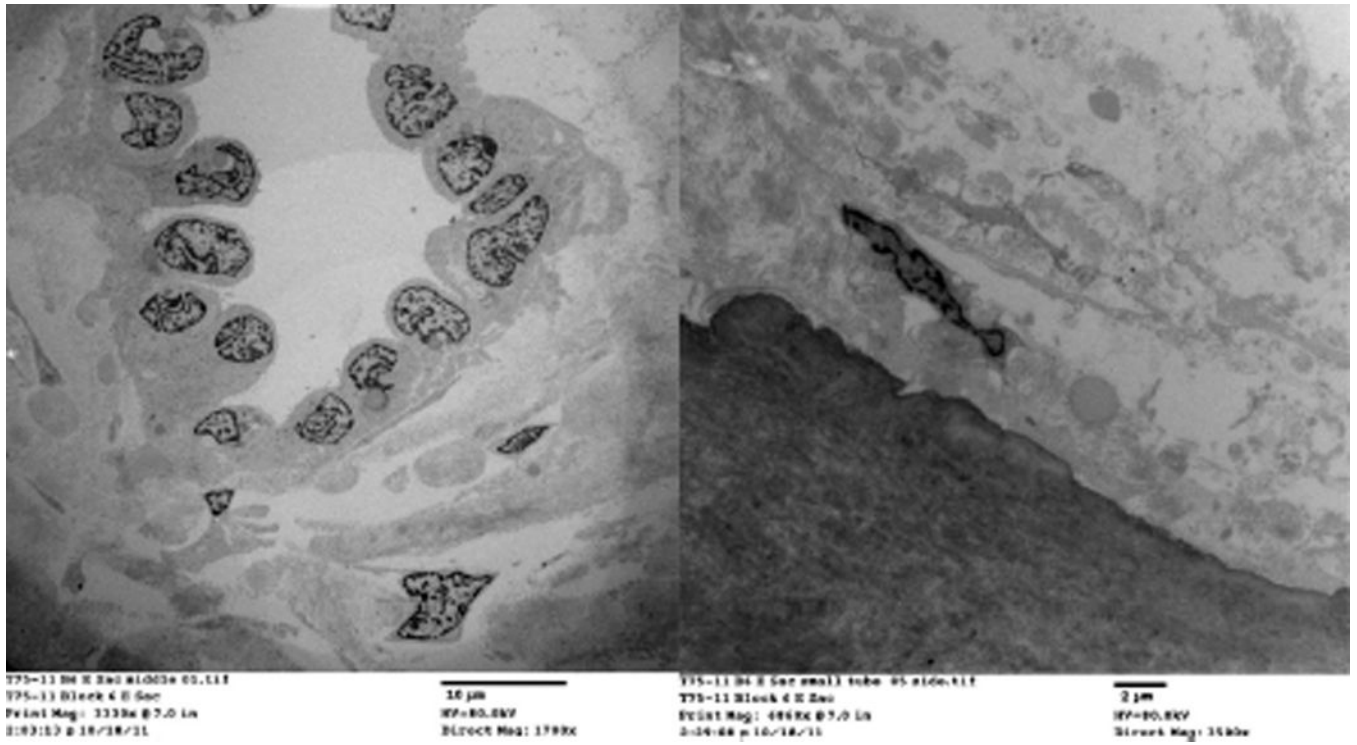


Figure 8.
 Electron microscopic images of similar fibroblasts in tissue around endolymphatic duct and in a periductal channel.

Table 1

Obstructed endolymphatic ducts.

Case Number	Age	Sex	Ear	Affected Ear	PTA	HT Interval Yrs	Vertigo Attacks	Unsteady	Hydrops Cochlea	Saccular	Etiology
103	64	M	R	R	65	3	No	Yes	Yes	Yes	Syphilitic gumma
			L	L	63				Yes	Yes	Syphilitic gumma
206	62	F	R	R	105	7	Yes		Yes	Yes	Syphilitic gumma
			L	L	38				Yes	Yes	Syphilitic gumma
366	54	F	R	R	Unknown	Unknown	Unknown		Yes	Yes	Syphilitic gumma
			L	L	Unknown	Unknown	Unknown		Yes	Yes	Syphilitic gumma
605	74	F	R	R	12	18	Yes		No	No	Normal
			L	L	85				Yes	Yes	Idiopathic fibrosis
632	42	M	R	L	Deaf	1	Yes		Yes	Yes	Idiopathic fibrosis
			L	L	Deaf				Yes	Yes	Idiopathic fibrosis
712	94	F	R	R	59	12		Yes	Yes	Yes	Scarlet fever
			L	L	43				No	No	Idiopathic
761	87	F	R	R	Deaf	0.75		Yes	Yes	Yes	Idiopathic
			L	L	Deaf				Yes	Yes	Idiopathic
1002	29	F	R	R	Deaf	0.1	No	No	Yes	Yes	Osteoma
			L	L	Deaf				No	No	Idiopathic
									Destroyed End Lymph Sacs		
39	71	M	R	R	20	0.5	No	No	No	No	Skull base osteomyelitis
			L	L	27				No	No	Malignant otitis externa
251	51	F	R	R	8		No	No			Not obtained
			L	L	98	0.08			No	No	Squamous cell carcinoma
258	19	M	R	R	17	0.6	Yes		No	No	Vestibular nerve schwannoma
			L	L	Deaf				No	No	Retrolabyrinthine NF2 schwannoma removal
736	74	M	R	R	Deaf	0.5	No	No	No	No	Neuron loss from scarlet fever
			L	L	125						Scarlet fever and otosclerosis

Abbreviations: End, endolymphatic; F, female; HT, hearing test; L, left; M, male; PTA, pure tone average; R, right; Yrs, years.

Table 2

Endo duct length.

Ménière's		Control	
Case Number	Duct Length in mm	Case Number	Duct Length in mm
273R	1.98	328L	1.09
384R	1.65	328R	2.1
409L	1.7	657L	2.2
409R	1.3	660R	2.04
403L	2.12	179L	1.35
453R	1.52	229L	1.51
594L	1.59	163R	2.31
236L	1.6	175R	1.5
230R	1.26	175L	1.37
Average	1.64	Average	1.72
SD	0.28	SD	0.44